EROSIONAL DEVELOPMENT OF BEDROCK SPUR AND GULLY TOPOGRAPHY IN THE VALLES MARINERIS, MARS

by

Peter C. Patton

Department of Earth and Environmental Sciences
Wesleyan University
Middletown, CT 06457

Final Report for NASA Grant NAGW-0244

ABSTRACT

Gully networks separated by resistant bedrock spurs are a common erosional feature along the escarpments that border the Valles Marineris. The resistant spur topography is best developed where the base of the slope is truncated by linear scarps interpreted as fault scarps. Regional variations in slope morphology imply that spur and gully topography undergoes a systematic progressive degradation through time associated with the erosional destruction of the basal fault scarps. The comparative morphometry of the divide networks indicates that the density of the spur networks and the number of first-order unbranched spurs decreases as the basal slope break becomes more sinuous. Abstraction of the spurs occurs through regolith storage in adjacent gullies at the slope base and the most degraded slope forms are entirely buried in talus. The basal fault scarps apparently control regolith transport by allowing debris to drain from the slope. As these basal scarps decay the slope base becomes increasingly sinuous and the slopes become transport limited. Dry mass-wasting may be the most important process acting on these slopes where a continually lowered base level is required to maintain the spur topography. In contrast to the martian slopes, range front fault escarpments in the western U. S. show no systematic trend in spur network geometry as they are eroded. These weathering limited slopes are controlled by the more efficient removal of regolith through fluvial processes which rapidly create quasi-equilibrium drainage

networks.

INTRODUCTION

The escarpments of the Valles Marineris (Fig. 1) display a range of slope forms from relatively straight undegraded slopes typical of Noctis Labyrinthus to the highly embayed eroded slope forms characteristic of the eastern chasmata (Blasius and others, 1977). Mass wasting and sapping processes have been most commonly invoked to explain the development of Valles Marineris scarp forms. Features interpreted to result from mass wasting include enormous landslides, similar to large rock avalanches or sturzstroms on Earth (Lucchitta, 1979); smaller scale slumps, retrogressive slides, and talus cones (Sharp and Malin, 1975; Blasius and others, 1977; Lucchitta, 1979); and small enclosed pits of probable subsidence origin (Baskerville, 1982; Steiner and others, 1982). Forms attributed to sapping include the branching theater-headed valleys prominent in Ius Chasma and smaller unbranched features throughout the Valles Marineris (Laity and Saunders, 1981; Kochel and Capar, 1982). In many instances the scarp morphology has been modified by the development of spur and gully topography (Lucchitta, 1978) which consists of erosional gullies separated by more resistant bedrock spurs. Spur and gully topography has been attributed to dry mass wasting (Blasius and others, 1977; Lucchitta, 1978) and more recently to fluvial erosion under past climatic conditions (Lucchitta, 1982).

Many of the slope forms are associated with tectonic

features. Some slope features are preferentially developed along structural lineaments while others appear to be modified by later structures. Examples of the former include chain craters and theater-headed valleys which often follow fractures and small grabens on the upland surface (Kochel and Capar, 1982). Examples of the latter are straight cliffs, interpreted as fault scarps (Blasius and others, 1977) which truncate the spur and gully topography near the base of several chasma walls. Horizontal resistant layers visible as terraces, lines of knobs and albedo bands in the upper portions of some chasma walls, may delineate lithologic variations. Although Blasius and others (1977) have suggested that spurs which descend from plateau crest to canyon floor and cross these layers provide evidence for the uniform erosional characteristics of the exposed lithologic units; regional variation in slope form may reflect differences in the stratigraphy of the chasmata walls.

The lack of craters on the floor of the Valles Marineris indicates that resurfacing of the canyon bottom has been an on-going process throughout the evolution of the canyon system (Blasius and others, 1977). The bulk of the chasmata floor sediment has probably been derived from the wall scarps and the rates and processes of sediment transport have undoubtedly varied over time. For example, Lucchitta (1979) has suggested, based on crater frequency statistics, that the most recent period of landsliding in the canyon system was contemporaneous with the last major period of volcanism is the Tharsis region. The lack

of erosional modification of the landslide scarps can be interpreted as evidence for the relatively recent occurrence of the slides (Lucchitta, 1979). Therefore, an investigation of slope forms within Valles Marineris is of value in determining both past and present surficial processes acting on the martian landscape and the relative influence of tectonics, structure and lithology on martian landform development.

The purpose of this study is to describe an evolutionary model for the development of the spur and gully topography and to discuss the significance of this model for erosional processes within the Valles Marineris. The spur and gully topography was chosen as the focus of this study for several reasons. It is a common slope form that is well displayed along the entire length of the Valles Marineris. The spur and gully forms have been attributed to non-catastrophic erosion and therefore may represent long-term landform development on Mars. Finally, the resistant bedrock spurs distinctive in map view, are easily resolved on the Viking imagery, and as will be demonstrated appear to be sensitive indicators of sediment transport and storage on these slopes.

EVOLUTION OF SPUR AND GULLY TOPOGRAPHY

Hillslope Models

Common models created to explain the evolution of hillslopes developed on fractured bedrock provide a starting point for evaluation of martian slope forms. Models which use the diffusion equation derived from the continuity expression for

transport on hillslopes (Kirkby, 1971) can accurately predict cliff retreat and slope form through time (Colman and Watson, 1983). However these models are dependent on an accurate estimate of the rate coefficient for slope processes (Colman and Watson, 1983) and are not appropriate for the proposed analysis. Since remote sensing imagery constitutes the data base for the martian landscape, more qualitative models are most appropriate for analyzing slope evolution. Through application of these qualitative models, slope morphology can be used to constrain the range of processes acting on the martian landscape.

The common evolutionary slope models can be divided into two end members based on the relative amount of sediment transported off the slope base compared to the volume of regolith produced along the slope profile. At one end member all debris produced on the slope, regardless of the weathering and erosion processes, is transported down the slope and off the slope base. This results in parallel retreat and continued exposure of bedrock on the slope profile (Fig. 2a) (Carson and Kirkby, 1972). Continued parallel retreat of an escarpment requires a balance between the rate of debris production and the sediment transport rate with only limited temporary regolith storage on the slope.

At the opposite end member little or no debris removal occurs and the slope gradually becomes stabilized as it is buried with regolith. Sediment production declines as the area of the scarp face diminishes and eventually a straight slope is produced at the angle of repose of the talus (Fig. 2c). This

configuration will remain stable until 1) conditions change at the slope base or crest, 2) weathering processes alter the regolith sufficiently to allow debris removal under the prevailing conditions or 3) the transport processes change (Carson and Kirkby, 1972).

A broad spectrum of slope profiles exists where either the nature of the transport processes at the slope base varies through time or the rate of sediment transport varies as the distance of transport increases across the lengthening slope. In this case the initial parallel retreat of the hillslope may give way to sediment storage and talus accumulation at the slope base (Fig. 2b). This process can eventually produce a talus mantle which will effectively buttress the hillslope and prevent further slope retreat. Although the final form is similar to the case of no sediment transport, the underlying bedrock profile is significantly different. The end member models outlined above can be traced to the original concepts of weathering and transport limited slopes described by Gilbert (1877).

Application of Slope Models to Spur and Gully Topography

Spur and gully morphology within the Valles Marineris can be interpreted in light of the previously described slope models. The major assumption made in this study is that the spatial variability in spur and gully morphology observed on the images represent geomorphic change through time. When geographically limited samples are consider the space for time assumption is a useful tactic for analyzing slope development (Craig, 1982).

Conversely, this assumption is probably invalid when the entire Valles Marineris is considered because the chasmata cross-cut three major geologic provinces that reflect a complex tectonic evolution which spans a long period of martian history. Thus, the escarpments have evolved for different lengths of time on different lithologic units presumably under different climatic regimes.

The progressive change in spur and gully topography developed along the length of the northern escarpment of Ius Chasma where it cuts the cratered plateau material (Fig. 1) can be interpreted as slope development through time. The observed changes can be attributed to the sediment transport and regolith storage processes on the various slope segments. At the eastern end of Ius Chasma the spur and gully topography is well developed on a canyon wall whose slope base abruptly terminates against a straight basal scarp (Fig. 3), interpreted by Blasius and others (1977) as a fault scarp. Similar to fault scarps on Earth, this scarp is relatively straight and characterized by well defined faceted spurs. The high density of bedrock spurs on this slope segment suggests that regolith storage is not significant and that sediment transport off the slope must be an efficient process. This slope would conform to the end member slope model of no regolith storage (Fig. 2a). It has been suggested that the lowered base level of the slope, caused by faulting, has been an important control in regolith transport from this slope (Blasius and others, 1977; Patton, 1981, 1982). The process might be dry

mass wasting of talus from the upper slope onto the floor of the chasma.

Approximately 250 km farther west in Ius, spur and gully topography appears more subdued with a lower density of bedrock spurs (Fig. 4). Spurs are shorter, only the major spurs extend to the base of the slope, and there appears to be a significant talus accumulation about the slope base. The lack of a basal fault scarp results in a more sinuous slope base. The crest of the slope is also more sinuous, the result of unequal headward erosion into the plateau surface. These slopes would conform to the idealized regolith storage hillslope form illustrated in Figure 2c. Thus the range in spur and gully forms along the chasma can be identified as stages in the evolution from weathering limited (Fig. 2a) to transport limited (Fig. 2c).

Coincident with the more degraded spur forms is an increased sinuosity of the contact between the escarpment and the valley floor. On Earth increased escarpment sinuosity with progressive erosion has been correlated with decreased tectonic activity for the fault bounded mountain ranges in the Basin and Range Province of the western United States (Bull and McFadden, 1977). A similar analogy to the cliffs along the Valles Marineris implies that there may be an interrelationship between escarpment sinuosity, tectonic activity, and the erosion and transport processes responsible for the development of the spur and gully topography.

Spur and Gully Morphometry

The evolution of spur and gully topography can be analyzed more precisely by measuring the attributes of these branching networks in the same manner that stream networks have been quantitatively described (Strahler, 1957; Shreve, 1966). In the analysis of the spur and gully topography, the spatial distribution and attributes of the spur topography were analyzed. This was done because the length, number and density of bedrock spurs appear to be most sensitive to either sediment transport or storage. In addition, the spur topography is well defined on the images and lent itself to measurement. Werner (1972) has demonstrated that divide or ridge networks can be topologically similar to stream networks within certain constraints on the linkage of ridge networks. Specifically, because each spur network in this analysis was rooted at the slope crest, the more complex spatial arrangements related to multiple ridge peaks and saddles (Mark, 1979) were eliminated. Thus the spur networks should be strongly related to the intervening gully systems.

The analysis of the spur or divide networks was accomplished as follows. Spur networks were mapped from orthographic images. Each network was defined by a master spur that intersected the slope crest. The spur networks branched down slope with each network defined by the major gullies on either side which head at the slope crest and the break in slope at the escarpment base. Spur networks were ordered by adopting the stream network ordering system of Strahler (1957) (Fig. 6). The following attributes of the slope network were measured: slope network area

(NA), slope network length (NL), total number of spurs of a given order n (M_n), and total length of all spurs in a slope network (SL). In addition, the average length of spurs of order n (L_n); spur density (DS), where:

$$DS = SL / NA \quad (1)$$

and spur frequency per unit area for a given order (FMn), where:

$$Fm_n = Mn / NA \quad (2)$$

were calculated.

Candor Chasma An analysis was made of all the slope networks in eastern Candor Chasma (Fig. 7) from a mosaic assembled from orthographic images at a scale of 1:280,000. A spatially limited sample was selected to reduce the effect that regional lithologic variation might have on slope form and development. In eastern Candor Chasma, the escarpments expose the ridged plains material, presumably, flood basalts, on both sides of the trough (McCauley, 1978). In the vicinity of eastern Candor, the ridged plains materials are estimated to be about 1 km thick (DeHon, 1982), which is substantially less than the height of the escarpment. Therefore, the underlying cratered plateau material (McCauley, 1978) must be exposed in the escarpment but no clear lithologic variation can be seen on the images.

The spur and gully networks on the southern wall of Candor Chasma offer an excellent contrast with those on the northern margin. The northern escarpment terminates against a basal fault scarp and the trace of the slope base is fairly straight with an average sinuosity of 1.3. The southern escarpment has a more

embayed base, no visible trace of a fault scarp and the slope base has an average sinuosity of 1.7. On the northern wall, 111 spur networks were identified, whereas over approximately the same distance, only 67 networks were mapped on the southern margin. In part, this is the result of the relatively smooth appearance of large segments of the southern escarpment. But also, network spacing, the scarp length divided by the number of networks (Wallace, 1978), is greater on the southern side of the chasma. The greater crest line and slope base sinuosity for the southern escarpment is evidence of more degradation (Bull and McFadden, 1977).

Network statistics indicate the following differences between northern and southern scarps (Table I). First, the average number of first-order spurs, the furthest downslope unbranched spurs, on the northern side of the chasma is greater and has a larger standard deviation than the first order spurs on the southern scarp (Table I). In contrast, the average length of first order spurs is greater on the southern wall. The first order spur statistics indicate that for the southern scarp either shorter erosional spurs have not developed along the downslope margin of the scarp or that preexisting first-order spurs have been buried. Burial of the first order spurs would convert longer, higher order spurs to first order spurs. In either case the results suggest a less efficient sediment transport regime on that chasma wall. Although the average number and length of higher order spurs per basin does not vary significantly between

scarps, the average spur density is greater on the northern scarp, presumably because of the increased number of first order spurs. In contrast the average length of the spur networks is slightly larger on the southern scarp but otherwise the statistics for network size are similar on both sides of the chasma.

Regression statistics illustrate the interrelationships between the morphometric variables and highlight the important differences between the two escarpments (Table II). The equations can also be interpreted in terms of spur network development. For example, network length increase as the square root of network area (equation 1, Table II). This indicates that divide networks should grow in width at an equal rate as they elongate. This also implies that the intervening gully systems must widen through time by the capture of adjacent basins. Eventually fewer, but larger, basins, should develop along an escarpment and with unequal headward growth, a more sinuous slope crest should develop. This conclusion is partly supported by the observations of increased network spacing for the southern escarpment.

Total spur network length is strongly controlled by network size (equation 2, Table II) and both northern and southern network populations have similar relationships, although total spur length increases at a greater rate with network area for the northern scarp. The significant difference in the slope of the regression lines is the result of the interdependence of total

spur length, network area, and the number of first order spurs. This interrelationship is documented by the regression equations relating the number of first order spurs to both network area and total spur length (equations 3, 4; Table II). Therefore the greater number and frequency of first order spurs on the northern wall is the significant difference between the two populations. The combined statistical data support the general model of escarpment evolution. First-order spurs which reflect the sediment transport efficiency of the intervening gullies increase at the greatest rate on the slopes with basal fault scarps. The fewer, but generally longer, first-order spurs on the southern escarpment are the result of the lack of development or the abstraction of pre-existing first order spurs caused by talus storage along the base of the slope system.

Regional Analysis

Slope networks were measured throughout the Valles Marineris to examine the stability and geographic applicability of the relationships developed for Candor Chasma. Over 600 networks were mapped and of these, 508 were classified as either terminating along a basal fault scarp or simply merging with the valley floor. Networks which terminated against landslide deposits derived from the opposite chasma margin were excluded from the analysis since they represent a third category. Several networks, mapped at a scale of 1:750,000, were excluded since scale dependent differences in resolution would have biased the sample. The final data set included 462 networks nearly evenly

distributed between the two sub-populations.

Regional network statistics display characteristics similar to the Candor networks. Networks which terminate with basal fault scarps have significantly more first order spurs and greater spur densities than those networks which merge gradually with the chasma floor (Table II). The level of significance for the difference in the means of spur density is lower for the regional data set and the level of significance remains the same in several cases where the numerical difference between means has decreased, an artifact of the increased population size (Snedecor and Cochran, 1967). The regression analysis for this larger data set revealed the same trends and significant differences between sub-populations, but the coefficients of determination are generally lower (Table III).

There are probably several reasons for the lower significance of these regression equations and the convergence of the network statistics. First, the process of scarp degradation is continuous and any attempt to analyze it through the use of two end member populations masks the range of slope forms present throughout the Valles Marineris. Second, it is reasonable to expect differences in escarpment development as a function of the lithology and age of the slope; and in the nature and rate of slope processes that might be controlled by these two variables. Therefore, when considering the entire Valles Marineris, the original assumption involving space for time substitution must be modified to incorporate these other factors. Detailed geomorphic

mapping is being used to define a more realistic stratification of this larger data set.

ANALOGY WITH FAULT SCARPS ON EARTH

The erosional development of the escarpments along the Valles Marineris can be compared to large tectonically created scarps on Earth. The concepts and general models for the geomorphic development of large fault scarps on Earth can be traced to the early work by Davis (1912) and Cotton (1917). More recent studies have focused on quantifying these earlier ideas and determining the interrelationships between tectonic activity and the resulting landforms along a mountain front (Bull and McFadden, 1977; Wallace, 1978). These studies have shown that, on Earth, dissection of fault scarps develops through the headward erosion of streams which create triangular facets along the fault scarp and narrow elongate drainage basins in the uplifted block (Cotton, 1917; Hamblin, 1976; Wallace, 1978). With continued dissection of the range front and unequal slope retreat along the fault scarp the mountain front becomes increasingly sinuous (Bull and McFadden, 1977; Wallace, 1978). Wallace (1978) has suggested that in the Basin and Range Province fault scarps and the associated debris covered slopes may persist for time periods on the order of 10^5 years while the associated erosional spur topography may last from 10^5 to 10^7 years.

There are several important parallels to the escarpments along the Valles Marineris. First, the hypothesized fault scarps in the Valles Marineris have the same morphology as those on

Earth with a low sinuosity surface expression, faceted spurs and relatively narrow elongate gully systems developed on the uplifted scarp. Second, there is an increase in sinuosity of the scarp base associated with the erosional decay of the overall escarpment. Finally, as demonstrated in Candor Chasma, the network spacing and lateral growth of the gully systems occurs concomitantly with the decay of the scarp.

To compare martian spur and gully topography with that developed on mountain fronts on Earth, the escarpments about three mountain ranges in the Basin and Range Province were analyzed in the same fashion as the scarps in the Valles Marineris. Range fronts analyzed were those along the Panamint, Tobin and Humbolt Ranges in California and Nevada. Based on the work by prior investigators, the range fronts were subdivided into either tectonically active range fronts with straight basal fault scarps or embayed degraded inactive range fronts (Bull and McFadden, 1977; Wallace, 1978). The Landsat image of the Humbolt Range in northern Nevada illustrates the difference between the straight western range front that is truncated by a fault scarp and the more degraded eastern escarpment (Fig. 8). Spur and gully topography was interpreted from Landsat imagery at a scale of 1:125,000 and spur network statistics were computed. In general, when each range is viewed separately there is no consistent trend between spur networks associated with fresh undegraded fault scarps and adjacent more degraded range fronts. The most consistent result was that the frequency of first order

spurs, a variable that adjusts for unequal spur network size, either increased or remained constant with increased degradation of range fronts, in contrast to the result observed for the martian networks (Table IV). The lack of significant trends is the result of the high efficiency of fluvial processes on Earth causing progressive dissection and creating weathering limited slopes in this environment. Also, on Earth, fluvial dissection and creation of drainage nets and associated slope networks is geologically rapid. The end result is the creation of a quasi-equilibrium drainage network after which there is little change in network statistics (Leopold and Langbein, 1962). This result, which contrasts with the statistical data for the Valles Marineris further strengthens the hypothesis that non-fluvial processes must be responsible for the development of the spur and gully topography on Mars and is consistent with a model of slope evolution dependent on dry mass wasting. Also, the erosional efficiency of fluvial processes on Earth results in the rapid degradation of fault scarps whereas scarps on Mars, probably several orders of magnitude older (Wise and others, 1979), have not yet been destroyed by the slower dry mass wasting processes.

DISCUSSION

The statistical analysis of the Valles Marineris spur and gully topography supports the qualitative observation that bedrock spurs are more numerous on those slopes with basal fault scarps. In addition, the data confirm that the furthest downslope spurs are the most sensitive network elements and that

differences between sub-populations can be largely attributed to changes in the length and frequency of these spurs. This result supports the initial hypothesis that fault-scarp based slopes are probably weathering limited whereas those scarps that merge with the valley floor are more likely transport limited. The close correlation between highly developed spur topography and the basal fault scarps implies a causal relationship. This study concurs with Blasius and others (1977) that this evidence argues for dry mass wasting processes as the most important sediment transport process on these slopes. The analogy with fault scarps on Earth is further evidence that fluvial processes have been unimportant in the development of spur and gully topography. In addition, the analysis suggests that spur topography can develop under the prevailing climatic conditions on Mars if the proper structural geomorphic setting exists. This does not imply recent tectonism on Mars to create spur and gully topography, but more likely that this transport process and erosional gully development is exceedingly slow.

The hypothesis that dry mass wasting is the dominant process creating spur and gully topography can be further supported through observations of escarpments where spur and gully topography is not prominently developed. For example, spur and gully topography is not well developed on the erosional scarps created by large landslides. High resolution images indicate that only short bedrock ribs protrude near the crest of the scarp and that talus produced on these slopes has collected at the

slope base. Talus cones mantle the slope creating a profile which mimics the most extreme end member of transport limited slopes. One interpretation of this observation is that spur and gully topography dates to an earlier period of erosion on Mars and that these landslide scarps are more recent features (Lucchitta, 1982). An alternative hypothesis, consistent with the model presented in this paper, is that bedrock spurs cannot develop where regolith storage is the predominant process. Because the landslide deposit effectively traps all the regolith produced on the scarp, sediment transport off the slope base is impeded, a transport limited slope profile develops, and the underlying bedrock topography of the slope is buried.

Spur and gully topography is also generally absent from the walls of the theater-headed valleys of probable sapping origin. Regolith storage predominates in these valleys indicating that transport processes have not been efficient in these geomorphic settings for a long time period. Valleys created through sapping processes require the removal of regolith in order to grow headward. The lack of erosional topography on the walls of the sapped valley networks implies that these valleys are relict features formed when surface transport processes were more effective.

Finally, in addition to the importance of the local geomorphic setting in controlling the development of spur and gully topography, regional variability in scarp morphology within the Valles Marineris is probably a function of the age of the

escarpment, the regional differences in lithology, and the spatial and temporal variability in the surficial processes conditioned by climate change on Mars. Systematic mapping and morphometric analysis will help to further determine the relative importance of these factors.

REFERENCES CITED

Baskerville, C. A., 1982, Collapse: a mechanism for martian scarp retreat: NASA Tech. Memo. 85127, p. 244-252.

Blasius, K. R., Cutts, J. A., Guest, J. E., and Masursky, H., 1977, Geology of the Valles Marineris: First analysis of imaging from the Viking I orbiter primary mission: J. Geophys. Res., v. 82, p. 4067-4091.

Bull, W. B., and McFadden, L. D., 1977, Tectonic geomorphology north and south of the Garlock Fault, California: in Doehring, D. O., ed., Geomorphology in arid regions, Publications in Geomorphology, Binghamton, NY, p. 115-138.

Carson, M. A.,and Kirkby, M. J., 1972, Hillslope form and process: Cambridge University Press, London, 475 p.

Colman, S. M. and Watson, K., 1983, Ages estimated from a diffusion equation model for scarp degradation: Science v. 221, p. 263-265.

Cotton, C. A., 1917, Block mountains in New Zealand: American Journal of Science, v. 44, p. 249-293.

Craig, R. G., 1982, The ergodic principle in erosional models: in Thorn, C. E., ed., Space and time in geomorphology, Allen and Unwin, London, p. 81-115.

Davis, W. M., 1912, Nomenclature of surface forms on faulted structures: Geol. Soc. Am. Bull., v. 14, p. 187-216.

De Hon, R. A., 1982, Martian volcanic materials: preliminary thickness estimates in the eastern Tharsis region: J. Geophys. Res. v. 87, p. 9821-9828.

Gilbert, G. K., 1877, Report on the geology of the Henry Mountains: W. S. Geog. and Geol. Survey of the Rocky Mountain Region,

Hamblin, W. K., 1976, Patterns of displacement along the Wasatch fault: Geology, v. 4, p. 619-622.

Kirkby, M. j., 1971, Hillslope process-response models based on the continuity equation: Trans. Inst. Brit. Geog., Spec. Pub. no. 3, p. 15-30.

Kochel, R. C., and Capar, A. P., 1982, Structural control of sapping networks along Valles Marineris, Mars, NASA Tech. Memo. 85127, p. 297-299.

Laity, J. E., and Saunders, R. S., 1981, Sapping processes and the development of theatre-headed valleys: NASA Tech. Memo. 84211, p. 280-282.

Leopold. L. B., and Langbein, W. B., 1962, The concept of entropy in landscape evolution: U. S. Geological Survey Prof. Paper 500-A.

Lucchitta, B. K., 1978, Morphology of chasma walls, Mars, U. S. Geol. Survey, J. Research, v. 6, p. 651-662.

Lucchitta, B. K., 1979, Landslides in Valles Marineris, Mars: J. Geophys. Res. v. 84, p. 8097-8113.

Mark, D. M., 1979, Topology of ridge patterns: randomness and constraints: Geol. Soc. Am. Bull., v. 90, p. 164-172.

McCauley, J. F., 1978, Geologic map of the Coprates Quadrangle of Mars: U. S. Geol. Survey, Map I-897 (MC-18), scale 1:5,000,000.

Patton. P. C., 1981, Evolution of the spur and gully topography on the Valles Marineris wall scarps: NASA Tech. Memo. 84211, p. 324-325.

Patton, P. C., 1982, Quantitative morphology of the Valles Marineris Scarps: NASA Tech. Memo. 85127, p. 242-243.

Sharp, R. P. and Malin, M. C., 1975, Channels on Mars: Geol. Soc. Am. Bull., v. 86, p. 593-609.

Shreve, R. L., 1966, Statistical law of stream numbers: J. Geology, v. 74, p. 17-37.

Snedecor, G. W. and Cochran, W. G., 1967, Statistical methods: Iowa State University Press, Ames, Iowa.

Steiner, J., Sodden, C., and Weiss, D., 1982, Aligned subsidence depressions in the vicinity of certain martian valleys: NASA Tech. Memo. 85127, p. 298-300.

Strahler, A. N., 1957, Quantitative analysis of watershed geomorphology: Trans. Am. Geophys. Union, v. 38, p. 913-920.

Wallace, R. E., 1978, Geometry and rates of change of fault-generated range fronts, north-central Nevada: U. S. Geol. Survey, J. Research, v. 6, p. 637-650.

Werner, C., 1972, Channel and ridge networks in drainage basins:

Assoc. Am. Geog. Proc. 4, p. 109-114.

Wise, D. U., Golombek, M. P., and McGill, G. E., 1979, Tectonic evolution of Mars: J. Geophys. Res. v. 84, p. 7934-7939.

LIST OF TABLES

LIST OF FIGURES

The position of the slope crest and base at various time intervals t_0, t_1, etc. are noted.

Figure 3. Spur and gully topography on the northern escarpment of eastern Ius Chasma. Note the basal fault scarp and the high density of bedrock spurs on the slope.

Figure 4. Spur and gully topography at the western end of Ius Chasma. The smooth slopes and the fewer bedrock spurs are the result of talus storage. Note the lack of a basal fault scarp and the slightly embayed slope base.

Figure 5. Highly embayed and degraded spur and gully topography at the western end of Ius Chasma. The plateau surface has been extensively eroded and only a few bedrock spurs extend to the slope base. Smooth slopes are the result of talus storage.

Figure 6. Simplified sketch of spur network geometry illustrating network boundaries and morphometric ordering.

Figure 7. Eastern end of Candor Chasma illustrating the basal fault scarp and the well developed spur and gully topography along the northern margin of the chasma. The southern margin of the trough has a more sinuous base and more degraded spur and gully topography.

Figure 8. Landsat image of the Humbolt Range in Nevada. Western side of the range terminates against a straight undegraded fault scarp. On the eastern side, erosion has obliterated the fault trace and the range front has a more sinuous contact with the piedmont.

Table I. Spur Network Statistics

	M_1	L_1	M_2	L_2	M_3	L_3	NA	NL	SL	DS	FM_1
	n	km	n	km	n	km	km^2	km	km	km^{-1}	n/km^2
N. Scarp Candor											
X	6.9**	1.8**	2.0	4.1	1.2	5.0	23.5	7.3*	17.3	0.9**	0.4**
s	9.1	1.0	1.8	3.0	0.5	3.6	31.9	4.8	22.5	0.6	0.3
n = 111											
S. Scarp Candor											
X	4.1**	2.8**	1.6	4.6	1.1	4.5	24.7	8.7*	14.5	0.7**	0.2**
s	3.6	2.0	0.9	3.3	0.5	3.8	23.6	4.4	12.0	0.2	0.2
n = 67											
Networks with Basal Scarps											
X	7.5**	2.0**	2.1	5.0	1.2	5.0	31.4	8.2	19.6	0.7*	0.3*
s	9.4	1.2	1.8	3.0	0.5	3.2	46.2	5.3	24.9	0.5	0.3
n = 221											
Networks merging with Chasma Floor											
X	5.4**	2.9**	1.7	5.1	1.1	6.1	38.4	9.3	18.6	0.6*	0.2*
s	7.0	2.0	1.3	3.5	0.4	5.0	55.4	5.9	23.2	0.3	0.2
n = 241											

X = mean
s = std. dev.

** Means significantly different at .01 level
* Means significantly different at .05 level

Table II. Regression Analysis of Network Parameters for Candor Chasma

	Region	Equation	R^2	F Ratio	Probability	Std. Error
1.	N. Candor	$NL = 1.83NA^{.49}$	.84	(1,109) = 572.77	.00001	.125
	S. Candor	$NL = 1.87NA^{.51}$	.89	(1,65) = 526.74	.00001	.084
2.	N. Candor	$SL = 1.0NA^{.89}$*	.90	(1,109) = 1015.63	.00001	.172
	S. Candor	$SL = 1.1NA^{.82}$*	.94	(1,65) = 944.39	.00001	.100
3.	N. Candor	$M_1 = .26NA + .65$*	.87	(1,109) = 713.28	.00001	3.31
	S. Candor	$M_1 = .13NA + 1.0$*	.71	(1,65) = 249.73	.00001	1.96
4.	N. Candor	$SL = 2.4M_1 + .58$*	.96	(1,109) = 2862.57	.00001	4.32
	S. Candor	$SL = 3.1M_1 + 1.76$*	.85	(1,65) = 354.33	.00001	4.74

* Regression line slopes significantly different at .01 level

Table III. Regression Analysis of Network Parameters for Valles Marineris

	Population	Equation	R^2	F Ratio	Probability	Std. Error
1.	Scarp	$NL = 1.70NA^{.49}$	.81	(1,219) = 922.81	.00001	.133
	Floor	$NL = 1.70NA^{.50}$	.83	(1,239) = 1211.90	.00001	.115
2.	Scarp	$SL = .85NA^{.90}$*	.86	(1,219) = 1442.91	.00001	.197
	Floor	$SL = .90NA^{.86}$*	.84	(1,239) = 1283.09	.00001	.186
3.	Scarp	$M_1 = .16NA + 2.3$*	.66	(1,219) = 428.45	.00001	5.46
	Floor	$M_1 = .10NA + 1.5$*	.64	(1,239) = 418.16	.00001	4.22
4.	Scarp	$SL = 2.5M_1 + .86$*	.89	(1,219) = 1854.39	.00001	8.11
	Floor	$SL = 3.1M_1 + 1.9$*	.87	(1,239) = 1652.82	.00001	8.26

Scarp = Networks which terminate against a basal fault scarp
Floor = Networks which merge with the chasma floor
* Regression line slopes significantly different at .01 level

Table IV. Spur network statistics for the Panamint, Humbolt and Tobin Ranges in the Basin and Range Province

		M_1	L_1	M_2	L_2	M_3	L_3	NA	NL	SL	DS	FM_1
		n	km	n	km	n	km	km^2	km	km	km^{-1}	n/km^2
Panamint Range												
Fault Scarp Range Front												
n=16	X	64.8	39.3	13.7	15.2	3.1	6.9	27.6	9.0	81.3	2.7	2.4
	s	49.3	31.3	9.9	12.1	2.2	3.7	19.1	4.9	86.7	1.1	.6
Degraded Range Front												
n=16	X	18.5	10.1	3.7	5.0	.7	3.9	6.5	4.1	16.9	3.0	4.1
	s	34.9	18.7	6.6	7.4	1.5	3.4	11.7	3.3	31.4	1.3	3.4
Humbolt Range												
Fault Scarp Range Front												
n=17	X	14.8	9.7	3.4	4.0	1.1	3.4	9.0	5.1	23.8	2.9	1.7
	s	8.1	5.1	1.9	2.0	.7	1.4	5.1	1.3	30.7	4.4	.5
Degraded Range Front												
n=24	X	20.2	12.0	4.7	4.8	1.2	3.6	11.7	4.9	20.0	1.7	1.7
	s	17.8	10.1	4.0	4.0	1.3	1.7	8.8	2.7	17.1	.5	.8
Tobin Range												
Fault Scarp Range Front												
n=31	X	13.3	7.1	2.6	2.9	.6	2.9	4.3	3.3	11.4	2.5	3.5
	s	14.6	10.0	2.7	3.2	1.0	1.7	4.8	1.7	14.7	1.3	2.3
Degraded Range Front												
n=21	X	17.7	9.2	3.3	3.8	1.0	2.4	5.7	3.6	14.6	2.6	3.4
	s	14.7	7.9	2.8	2.9	.9	1.7	4.6	1.6	13.1	.7	1.9

x = mean
s = standard deviation

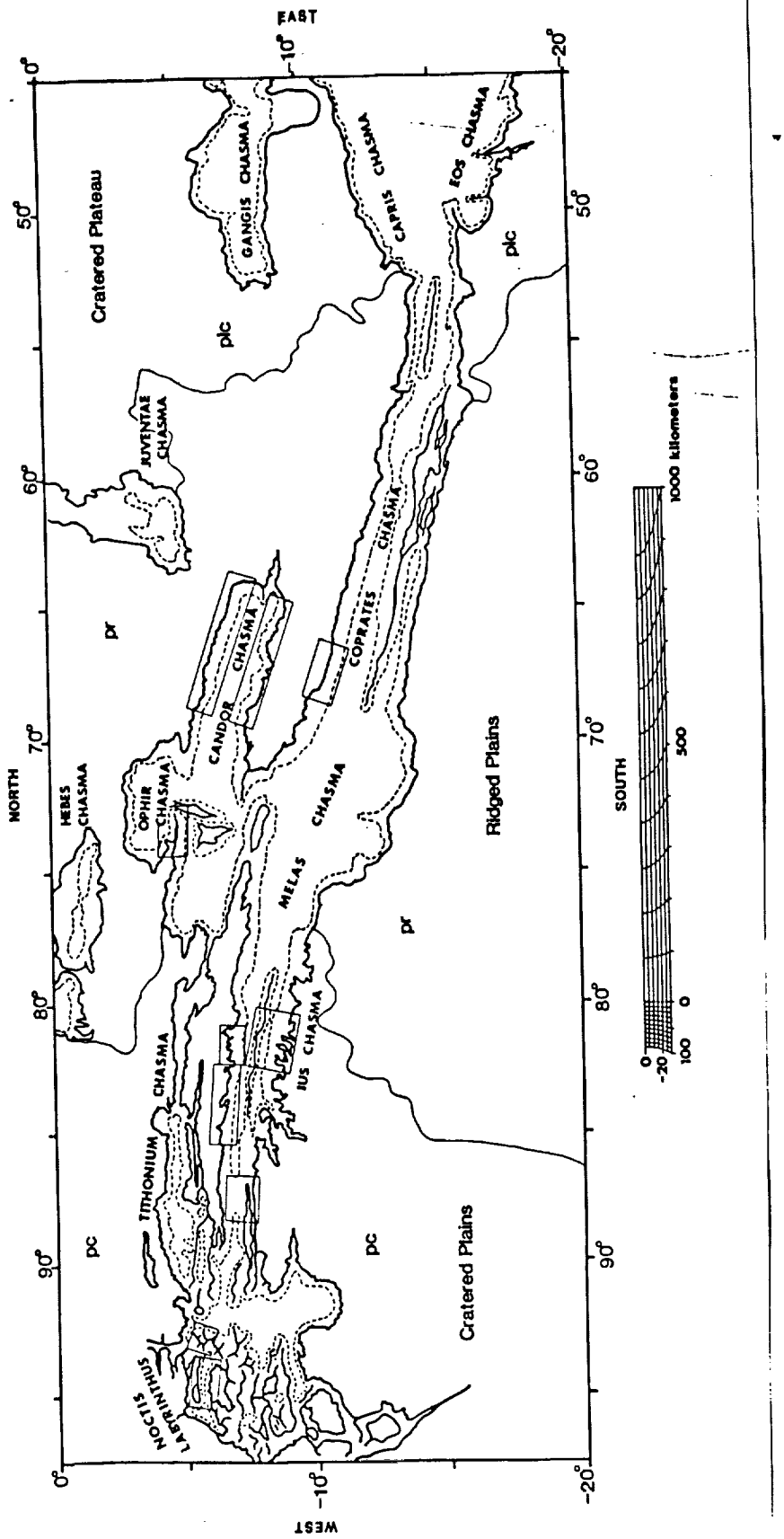

Figure 1

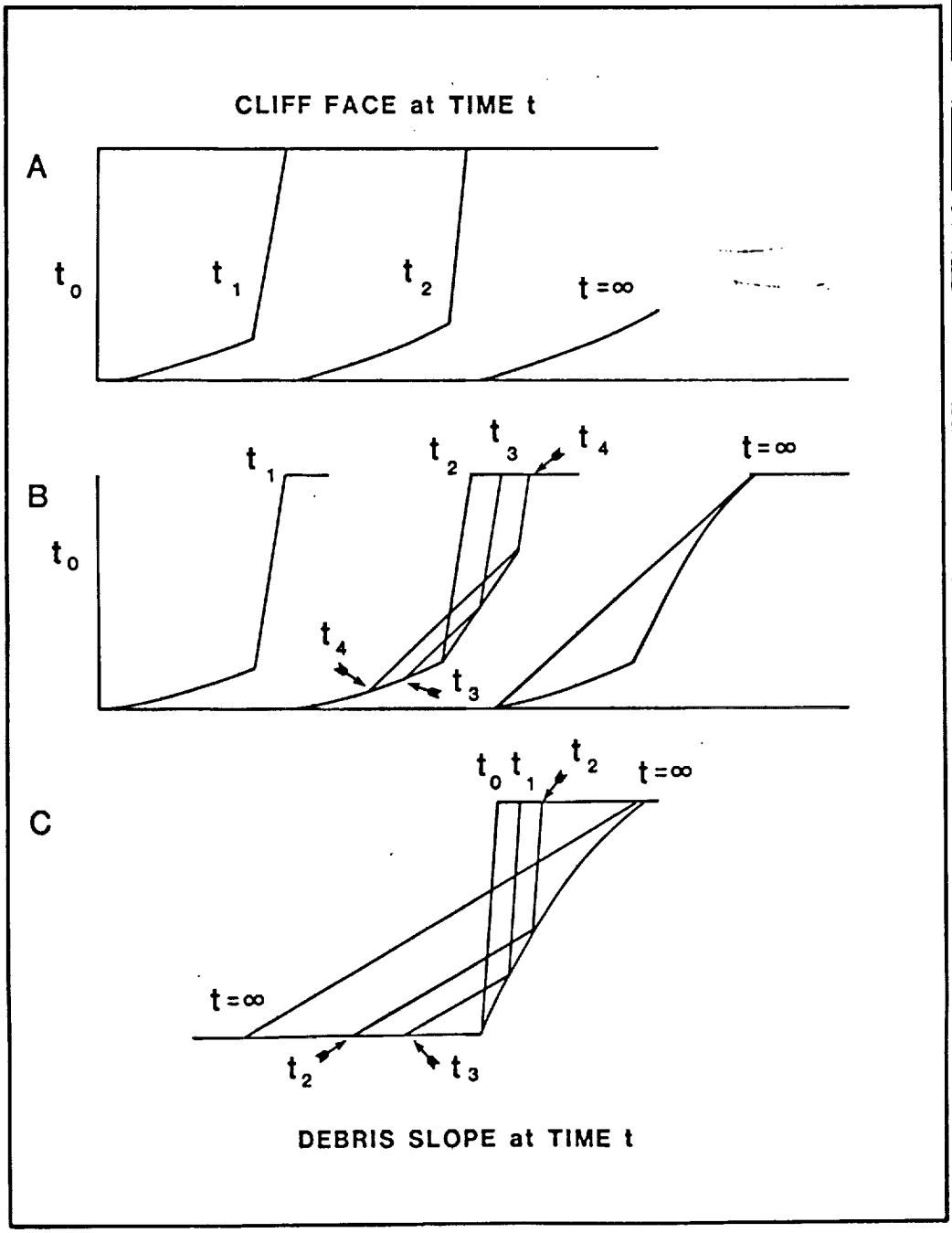
CLIFF FACE at TIME t
A
t_0
t_1
t_2
$t=\infty$
B
t_0
t_1
t_2
t_3
t_4
$t=\infty$
t_4
t_3
C
t_0 t_1
t_2
$t=\infty$
$t=\infty$
t_2
t_3
DEBRIS SLOPE at TIME t

Figure 2

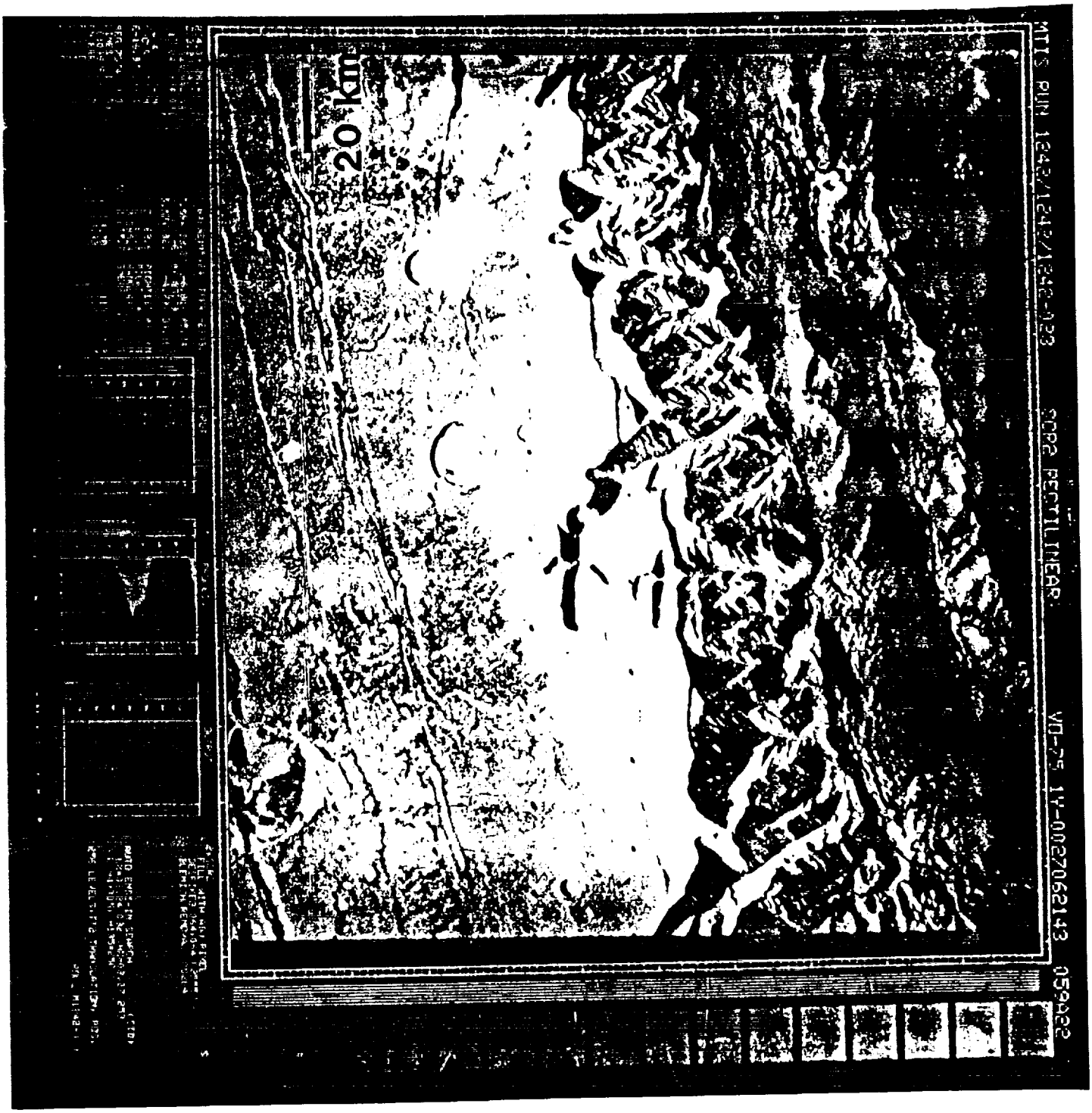

Figure 3

ORIGINAL PAGE IS
OF POOR QUALITY

ORIGINAL PAGE IS
OF POOR QUALITY

Figure 4

Figure 5

ORIGINAL PAGE IS
OF POOR QUALITY

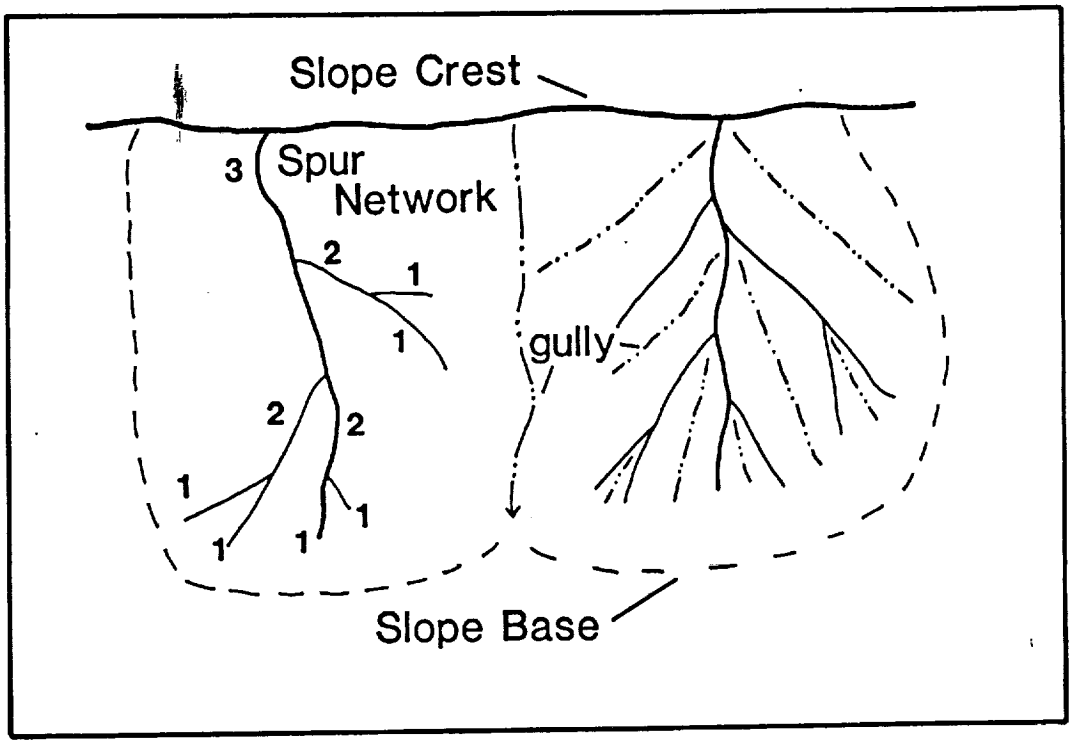

Figure 6

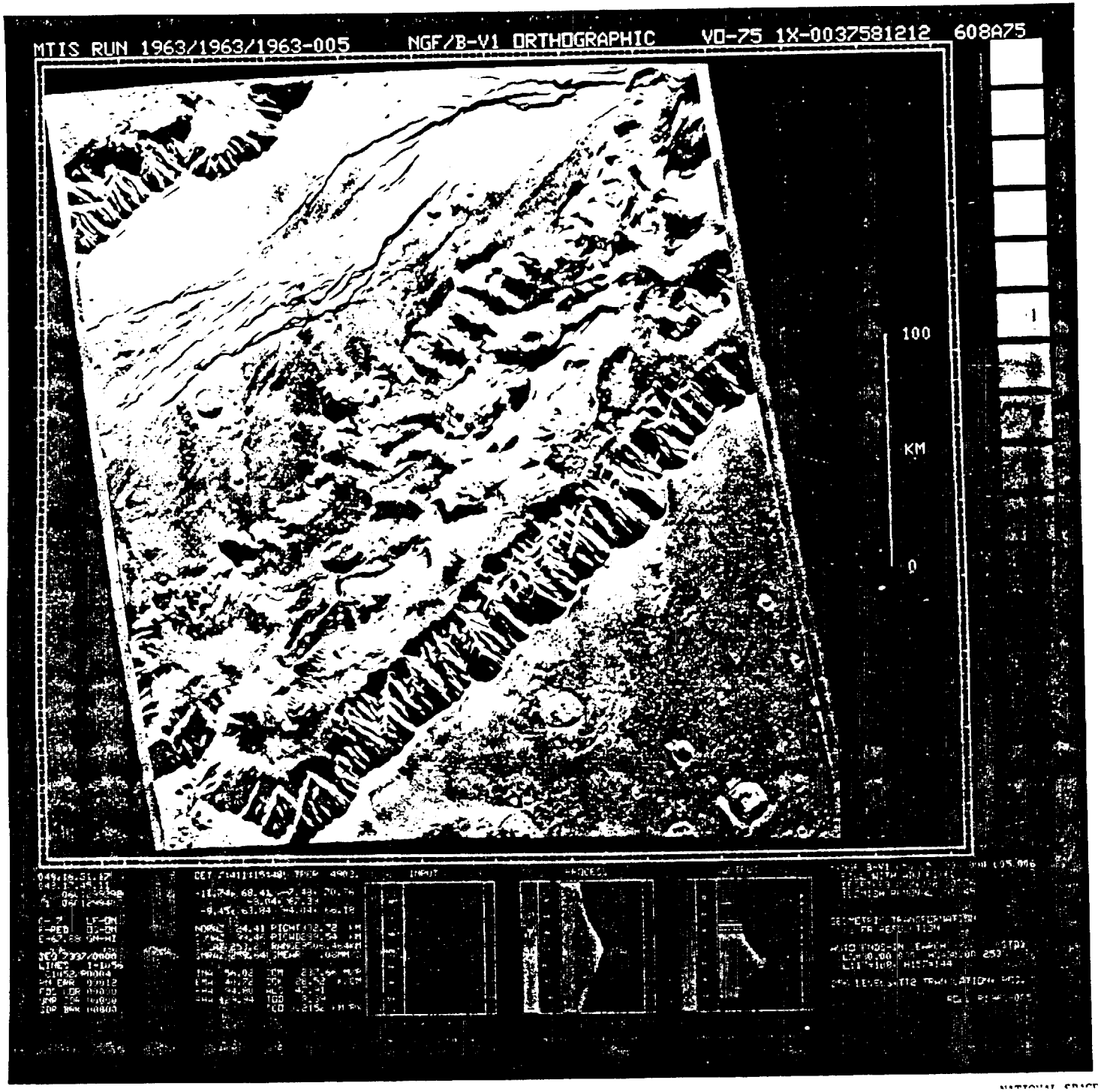

Figure 7

Figure 8